

2012

# Human muscle-derived cell populations isolated by differential adhesion rates: Phenotype and contribution to skeletal muscle regeneration in Mdx/SCID mice

Steven M. Chirieleison

*University of Pittsburgh - Main Campus*

Joseph M. Feduska

*University of Pittsburgh - Main Campus*

Rebecca C. Schugar

*Washington University School of Medicine in St. Louis*

Yuko Askew

*University of Pittsburgh - Main Campus*

Bridget M. Deasy

*University of Pittsburgh - Main Campus*

Follow this and additional works at: [http://digitalcommons.wustl.edu/open\\_access\\_pubs](http://digitalcommons.wustl.edu/open_access_pubs)

---

## Recommended Citation

Chirieleison, Steven M.; Feduska, Joseph M.; Schugar, Rebecca C.; Askew, Yuko; and Deasy, Bridget M., "Human muscle-derived cell populations isolated by differential adhesion rates: Phenotype and contribution to skeletal muscle regeneration in Mdx/SCID mice." *Tissue Engineering: Part A*.18,3-4. 232-241. (2012).  
[http://digitalcommons.wustl.edu/open\\_access\\_pubs/3278](http://digitalcommons.wustl.edu/open_access_pubs/3278)

# Human Muscle-Derived Cell Populations Isolated by Differential Adhesion Rates: Phenotype and Contribution to Skeletal Muscle Regeneration in Mdx/SCID Mice

Steven M. Chirieleison, B.S.,<sup>1,2</sup> Joseph M. Feduska, B.S.,<sup>1</sup> Rebecca C. Schugar, B.A.,<sup>1,3</sup>  
Yuko Askew, M.D., Ph.D.,<sup>1</sup> and Bridget M. Deasy, Ph.D.<sup>1,4,5</sup>

Muscle-derived stem cells (MDSCs) isolated from murine skeletal tissue by the preplate method have displayed the capability to commit to the myogenic lineage and regenerate more efficiently than myoblasts in skeletal and cardiac muscle in murine Duchenne Muscular Dystrophy mice (*mdx*). However, until now, these studies have not been translated to human muscle cells. Here, we describe the isolation, by a preplate technique, of candidate human MDSCs, which exhibit myogenic and regenerative characteristics similar to their murine counterparts. Using the preplate isolation method, we compared cells that adhere faster to the flasks, preplate 2 (PP2), and cells that adhere slower, preplate 6 (PP6). The human PP6 cells express several markers of mesenchymal stem cells and are distinct from human PP2 (a myoblast-like population) based on their expression of CD146 and myogenic markers desmin and CD56. After transplantation to the gastrocnemius muscle of *mdx*/SCID mice, we observe significantly higher levels of PP6 cells participating in muscle regeneration as compared with the transplantation of PP2 cells. This study supports some previous findings related to mouse preplate cells, and also identifies some differences between mouse and human muscle preplate cells.

## Introduction

**D**UCHENNE MUSCULAR DYSTROPHY (DMD) is a muscle disease characterized by extensive and progressive muscle degeneration due to the lack of dystrophin protein expression at the sarcolemma of muscle fibers.<sup>1</sup> The lack of dystrophin at the membrane disrupts the structural connection between the cytoskeleton and the extracellular matrix, thus resulting in muscle fiber necrosis and weakness.<sup>2,3</sup> Onset of symptoms occurs early in childhood (between 2 and 6 years of age), and in recent years, survival has been improved to early adulthood by using approaches such as mechanical ventilation.<sup>4,5</sup> Effective treatment of DMD will likely require long-term replacement of the missing dystrophin protein. Muscle stem cells, such as satellite cells, are the resident postnatal, progenitor repair cells for skeletal muscle.<sup>6–8</sup> Due to the natural tendency of muscle progenitor cells to fuse with existing or newly forming muscle fibers, cell transplantation approaches to treating DMD are promising. Indeed, 20 years ago, Partridge *et al.* first showed that transplantation of normal myoblasts can restore dystrophin expression in dystrophin-deficient muscle of *mdx* host mice,<sup>9</sup> and this spurred enthusiasm for human clinical trials based

on this approach.<sup>8,10–13</sup> However, some studies exhibited limited success, and this was associated with host immune rejection, poor donor cell survival, proliferation and migration, and challenges in systemic delivery.

Although the transplantation of normal myoblasts restores dystrophin expression in some myofibers in *mdx* mice<sup>9,14–16</sup> and patients with DMD,<sup>10,17,18</sup> the use of less-committed muscle stem cells may improve the efficacy of this approach. Reports now describe the heterogeneity of muscle stem cells; in particular, a subset of satellite cells may be capable of repopulating the satellite pool,<sup>6,19</sup> or different progenitors may derive from interstitium or endothelial sources, for example<sup>7</sup>; and transplantation of these cells may lead to better muscle regeneration. A population of mouse muscle-derived stem cells (msMDSCs) with an undefined relationship to satellite cells has been described<sup>20,21</sup>; msMDSCs have stem cell characteristics that may help overcome hurdles associated with myoblast transplantation therapy. In particular, msMDSCs, isolated by a preplate method, exhibited an increased capacity for muscle regeneration in the *mdx* mice as compared with myoblasts.<sup>21</sup> The preplate-isolated msMDSCs also demonstrate long-term self-renewal and multi-lineage differentiation

<sup>1</sup>Stem Cell Research Center, University of Pittsburgh, Pittsburgh, Pennsylvania.

<sup>2</sup>Department of Biomedical Engineering, University of Texas, Austin, Texas.

<sup>3</sup>Center for Cardiovascular Research, Washington University School of Medicine, St. Louis, Missouri.

<sup>4</sup>Department of Bioengineering, Swanson School of Engineering, University of Pittsburgh, Pittsburgh, Pennsylvania.

<sup>5</sup>McGowan Institute for Regenerative Medicine, University of Pittsburgh Medical Center, Pittsburgh, Pennsylvania.

capability.<sup>21–23</sup> Extensive examination of msMDSCs have been performed to better understand how the isolation procedures selects for this population as well as how these cells are distinct from myoblasts and what may be their origins.<sup>21,24–30</sup> However, less work has been performed to determine whether this work can be translated to human cells and whether these cells can be isolated from human tissue by using the same method.

We and others have examined the regenerative efficiency of various human muscle stem cells isolated by fluorescence activated cell sorting (FACS) purification for skeletal muscle repair; however, no studies to date report on the human preplate-derived cells that would be a counterpart to the well-described msMDSC.<sup>31</sup> Recent work has focused on the isolation of progenitor cells associated with the human blood vessels, including CD34+CD144+CD56+ myogenic-endothelial cells,<sup>32</sup> CD146+ pericytes,<sup>7</sup> mesoangioblasts,<sup>33</sup> and CD133+ progenitor cells,<sup>34</sup> the latter of which was investigated in a recent phase I clinical trial.<sup>35</sup> In contrast to those discussed so far, the human skeletal MDSCs (hMDSCs) isolated by the preplate technique have yet to be examined for their *in vivo* myogenic repair capacity. Human muscle-derived cells have been isolated by the preplate technique from muscle tissue for several years,<sup>36–38</sup> however, examination of these cells in skeletal muscle regeneration models has not been performed.<sup>31</sup>

Here, we investigate human muscle-derived cells obtained by the preplate technique in transplantation studies using the mdx/SCID mice. We examine phenotypic differences and the regenerative potential of two specific populations of human muscle-derived cells isolated by differential adhesion rates during the preplate method—preplate 2 (PP2) cells which are faster to adhere, and preplate 6 (PP6) cells that are slower in adhering.

## Materials and Methods

### Cell isolation

Human muscle-derived cells were isolated by way of differential adhesion rates by using a modification of methods as previously described.<sup>21,39</sup> Human skeletal muscle was enzymatically digested by using collagenase, and dispase and serial preplating was performed to separate cell fractions preplate 1 (PP1), PP2, and preplate 3 (PP3) through to PP6. Cells that adhere to noncollagenated tissue culture plastic flasks within the first 30 min were PP1 cells. Medium and nonadhered cells from the PP1 flasks were then transferred to a fresh flask, and cells that adhered during 30 to 60 min were termed “PP2” flasks. Again, media and nonadhered cells were transferred to fresh flasks and allowed to adhere such that PP3 cells were those that adhered 1 to 2 h post-plating. PP4 cells adhered after 2 to 24 h, and PP5 cells adhered between 24 and 48 h. PP6 cells adhered between 48 and 120 h. During the isolation process, cells were grown in Dulbecco’s modified Eagle medium (Gibco) with 20% fetal bovine serum and 0.5% Chick Embryo Extract. Cells were then frozen for later use. For the current study, we compared the fast adhering cells from PP2 and slow adhering cells from PP6, which would be most comparable to msMDSCs.<sup>21</sup>

### Cell culture

Candidate populations were grown in EGM™-2 media (Lonza) at a density of 600–800 cells/cm<sup>2</sup> under standard

conditions (5.0% CO<sub>2</sub>, 37°C). Cells were passaged every 72–96 h by treatment with 0.05% trypsin (Invitrogen) diluted 1:1 in 1× Dubecco’s phosphate buffer solution (DPBS; Invitrogen) at 37°C for 3–4 min. Detached cells were then washed in 1× DPBS, centrifuged, and suspended in 1.0 mL of media for counting via hemocytometer.

### Flow cytometry analysis

PP6 and PP2 cells were analyzed for expression of cell surface cluster of differentiation markers CD34, CD73, CD90, CD146 (BD Pharmingen), CD44, CD105 (Invitrogen), CD56 (BioLegend), CD45, and CD144 (eBioscience) at the first three passages in culture. Cells were initially incubated in a blocking solution of 10% goat serum in DPBS (Vector) for 30 min on ice before primary antibody treatment. After primary antibody treatment, and secondary labeling with streptavidin-Allophycocyanin (BD Pharmingen) where appropriate, cells were washed, suspended in 300 μL of 1× PBS (Invitrogen), and fixed with 80 μL of 5% formalin. Flow cytometric acquisition and analysis was performed by using an FACSCalibur® (Becton Dickinson), and expression was determined as fluorescence emission levels exceeding 98% of unlabelled controls.

### Immunocytochemistry

PP6 and PP2 cells were plated in a 24-well plate at a density of 600–800 cells/cm<sup>2</sup>. After 72–96 h, cells were fixed with 100% cold methanol (Fisher), blocked in 10% horse serum in DPBS, labeled with either primary 1:250 mouse anti-desmin (Sigma) or mouse anti-Myosin Heavy Chain Fast (Sigma) antibody, followed by secondary labeling with 1:250 biotinylated goat anti-mouse IgG (Vector Laboratories), 1:500 streptavidin-Cy3 (Sigma); nuclei were counterstained with 300 nM 4'-6-diamidino-2-phenylindole (DAPI) (Invitrogen). After staining, images of cells were taken on a Nikon TE-2000-U microscope (Nikon Instruments) with Spot RT-ke camera and software (Diagnostic Instruments) and then quantified as desmin positive nuclei per total nuclei. Positive expression was determined by setting exposure using unlabelled controls.

### Bioinformatic live cell imaging

Although traditionally established tools such as flow cytometry and molecular methods are frequently used to characterize cells, the use of time-lapsed microscopy to reveal additional cell behaviors represents a novel method to characterize potentially therapeutic cells. In this study, we used a previously described method to measure a number of cell features from time-lapsed images.<sup>40–42</sup>

Cells seeded at 600–800 cells/cm<sup>2</sup> in a 24-well plate were incubated in a cell culture system with dynamic imaging.<sup>40</sup> Images were captured at 10-min intervals over 72–96 h. To measure mean cell area, we imported time-lapsed image sets to ImageJ (NIH), and at 5 different time points, 10 separate cells were traced over three consecutive frames, thus yielding 30 measurements per time point. Averaging mean cell area across time points yielded values for the population. Cell velocity was determined by tracking the location of cell centroid in three consecutive images, dividing distance change of centroid across consecutive frames by the time interval of 10 min between scans yielded

single cell velocity. Averaging 10 separate cell measurements at each time point and averaging time point values yielded cell velocity for each population. A similar method was used to find mean circularity.

### In vivo regeneration

For PP2 ( $n=3$  PP2 populations with a total of 18 muscles) and PP6 ( $n=3$  PP6 populations with a total of 26 muscles), 100,000 cells in 30  $\mu$ L PBS were transplanted to the gastrocnemius muscles of 8- to 10 week-old *mdx*/SCID mice. For control muscles, we also used (1) sham injections of 30  $\mu$ L PBS ( $n=4$ ) and (2) no transplantation or no injection *mdx*/SCID muscles ( $n=5$ ). Muscles were harvested 2 weeks post-transplantation and frozen sectioned into 10- $\mu$ m sections. Some serial sections were stained with hematoxylin and eosin; others were stained with specific antibodies. For immunohistochemical analysis, sections were blocked in 10% donkey serum in DPBS (Jackson ImmunoResearch), incubated in primary 1:200 rabbit polyclonal anti-mouse/anti-human dystrophin (Abcam, Cat #15277), followed by 1:250 Alexa Fluor 594 donkey anti-rabbit IgG (Invitrogen), and nuclei were counterstained with 300 nM DAPI (Invitrogen). Sections were then counted by visual inspection on a Nikon E800 (Nikon Instruments) with a 20 $\times$  objective for dystrophin positive fibers, and the greatest number of dystrophin positive fibers in a single muscle cross-section yielded the Regeneration Index, or number of dystrophin-positive fibers, for that muscle. For sham PBS-injected muscles and no-injection muscles, we quantified the number of revertant dystrophin positive fibers in the gastrocnemius cross-section. The regeneration index (RI) of cell transplantations and the number of revertant fibers in control muscles are plotted on the same graph in Figure 5 for ease of comparison. Centro-nucleation was quantified as the percentage of myofibers in a given section that show nuclei within the fiber center and clearly not peripheral. Fiber diameter and area were measured by using ImageJ (NIH) line and trace tools.

For detection of human dystrophin, slides were stained using the Vector M.O.M. Immunodetection Kit (Vector Laboratories) with 1:10 mouse anti-human dystrophin (DYS3; Novocastra) primary antibody, 1:250 biotinylated goat anti-mouse IgG secondary antibody (Vector Laboratories), and 1:500 streptavidin-Cy3 (Sigma); nuclei were counterstained with 300 nM DAPI (Invitrogen). Nuclei sex was confirmed by fluorescence *in situ* hybridization. Degenerate oligonucleotide-primed PCR-labeled Y probes were used to label the Y-specific nuclear antigen in nuclei of the male host mouse to visualize fusion with recipient fibers.

### Results and Discussion

Two human muscle-derived cell populations, separated at the time of isolation by their rates of adhesion, were obtained by a modified preplate technique.<sup>21,39</sup> The 2 populations were termed "PP2" (adhering within first hour) and "PP6" (adhering after 2–5 days), corresponding to their initial rate of adherence during the isolation procedure (Fig. 1). Previously, mouse myoblasts (fast adhering) could be separated from MDSCs (slowly adhering) based on adherence rates.<sup>21</sup>

We examined whether the human muscle-derived PP2 and PP6 populations might be further distinguished by

molecular surface marker phenotype and expression of the myogenic-related intermediate filament desmin. We performed flow cytometry for endothelial and blood-cell-related surface markers CD34, CD45, CD144, and CD146; mesenchymal stem cell-related surface markers CD44, CD73, CD90, and CD105; and the myogenic-related surface marker CD56 for the PP2 and PP6 populations. Both PP2 and PP6 populations were negative (<2%) for CD34, CD45, and CD144 and consistently, highly positive for mesenchymal markers (>95%) CD44, CD73, CD90, and CD105, thus exhibiting little variability between samples or across PP2 and PP6 populations (Fig. 2A). Slow adhering cells showed lower CD146 levels (Fig. 2B) and lower CD56 levels (Fig. 2B) as compared with PP2 cells (CD146: 31% vs. 64%, and CD56: 46% vs. 79%, respectively, PP2 populations not shown in Fig. 2). There is a significant positive correlation between the level of expression of CD146 and the myogenic marker CD56 in both PP6 and PP2 populations ( $p<0.05$ , Fig. 2C). We also observe lower levels of myogenic marker desmin by immunocytochemistry (in PP6 populations as compared with PP2 populations; 34% vs. 77%, Fig. 2D). In sum, PP2 and PP6 populations exhibited significant differences in the percentage of cells expressing CD146, CD56, and desmin (Fig. 2E,  $p<0.005$ ). Examination of mesenchymal markers was not previously performed for preplate-derived MDSC isolated from other species;<sup>43–50</sup> however, a study of CD56-sorted cells showed MSC markers CD90 and CD106 positivity on MDSCs from craniofacial muscles.<sup>51</sup> Our findings related to desmin and CD56 are consistent with murine myoblast and MDSC studies.<sup>21,22,48,52</sup>

Interestingly, the human PP2 and PP6 cells exhibited a few differences in proliferative characteristics related to their population doubling time (PDT), cell division time (DT), or mitotic fraction (Fig. 3A–C). The mean PDT for PP6 cells was 34 h, whereas the PDT for PP2 cells was 31 h (not significantly different, Fig. 3A). There was no significant difference in the cell cycle time, or DT, between PP6 and PP2 cells. These results are in contrast to the similar mouse muscle cell populations that showed faster DT in myoblasts as compared with msMDSCs<sup>21</sup>; however, it should be noted that myoblasts readily differentiate and fuse such that they have limited long-term expandability.<sup>21</sup> In addition, similar to the mouse populations, both human PP2 and PP6 populations exhibited morphological heterogeneity (Fig. 1); however, on average, the human PP6 cells displayed larger area or cell spreading in monolayer as compared with PP2 cells (Fig. 3D). Finally, we also examined the migration rates (although it has not been shown, *in vitro* migration capacity may relate to cell dispersion post transplantation) of the human muscle cell populations. We found that PP2 cells exhibited lower cell velocity as compared with PP6 cells (0.41 vs. 0.66  $\mu$ m/min); this had not been previously examined in mouse populations. A summary of comparisons between human and mouse PP2 and PP6 cells is provided in Supplementary Table T1; Supplementary Data are available online at [www.liebertonline.com/tea](http://www.liebertonline.com/tea).

We next examined myogenic activity of the PP2 and PP6 populations. Reverse Transcription polymerase chain reaction (RT-PCR) results showed the populations' expression of several myogenic markers—myf-5, myoD, and myogenin (Fig. 4A). RT-PCR analysis (Fig. 4A) also confirmed the expression of desmin and myosin as detected by



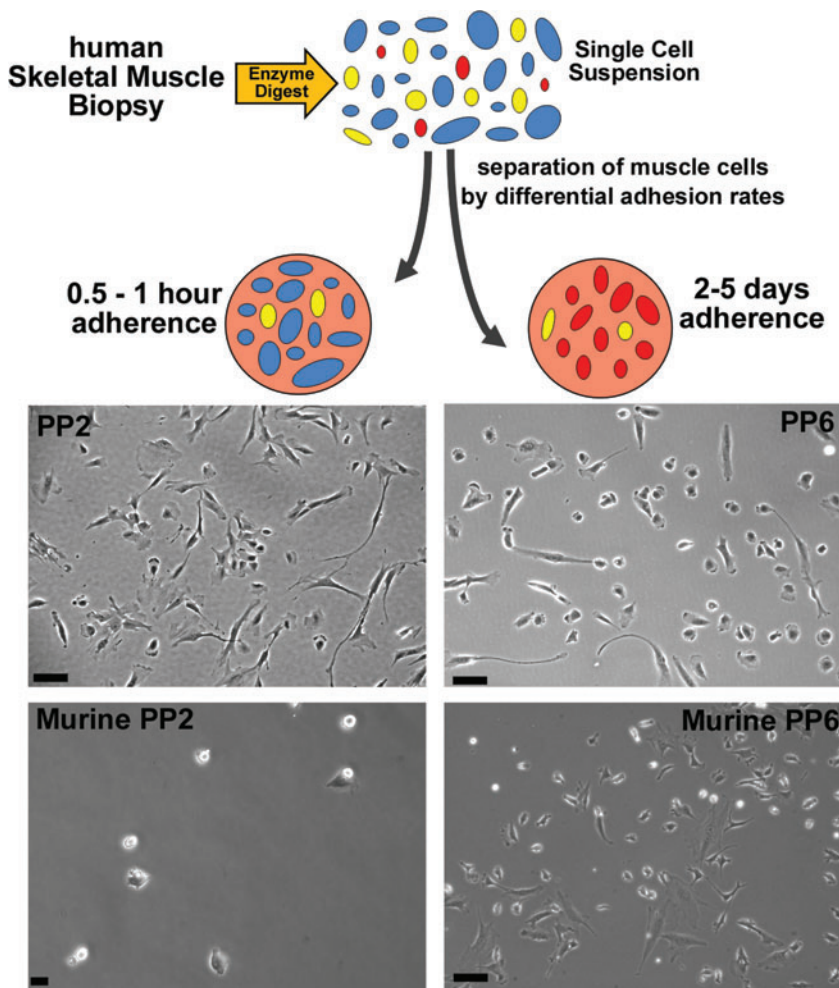


FIG. 1. Schematic isolation of human muscle cell populations. The human muscle biopsy is first enzymatically digested, and then, the cells are preplated on noncoated flasks. After separation of single-cell isolates by adherence rates, two main populations are acquired: PP2, fast adhering cells and PP6, slow adhering cells. Scale bars represent 100  $\mu\text{m}$ . PP2, preplate 2; PP6, preplate 6. Color images available online at [www.liebertonline.com/tea](http://www.liebertonline.com/tea)

immunohistochemistry; however, we did not detect clear significant differences in these markers by RT-PCR. In both PP2 and PP6 groups, there were populations that expressed the more differentiated markers myogenin and myosin, whereas some populations in these groups did not express these markers. Previously, others reported that mouse slowly adhering MDSCs expressed myoD,<sup>43,45</sup> and this was similar to the levels expressed by myoblasts.<sup>21</sup> Our findings, showing that a smaller percentage of human PP6 is desmin positive (34%), are consistent with a similar report by some of us in which msMDSC populations were ~15% desmin positive, and the mouse PP2 myoblast-like populations were >80% desmin positive.<sup>21</sup> However, several other reports show that desmin expression is high in MDSC populations.<sup>25,43,45,51</sup> Both PP2 and PP6 muscle cell populations exhibited the capacity to differentiate to the myogenic lineage as demonstrated by fast myosin heavy chain and multi-nucleate myotubes *in vitro* (Fig. 4B).

Since the most striking difference between mouse myoblasts and MDSCs was their *in vivo* regeneration capacity, we performed cell transplantations of the human PP2 and PP6 populations to gastrocnemius muscles of mdx/SCID mice. Two weeks after transplantation of 100,000 cells, we performed immunostaining for dystrophin in the cross-sections of muscle tissue. We quantified the RI as the mean number of dystrophin positive fibers per  $10^5$  donor cells. We detected centro-nucleated muscle fibers in both PP2 and

PP6-transplanted muscles (Fig. 5A, B, respectively), which corresponded with regions of dystrophin positive fibers (Fig. 5C, D). The mean RI after transplantation of PP6 ( $71 \pm 4$ ) was significantly higher than the mean RI after transplantation of PP2 ( $58 \pm 5$ ,  $p=0.046$ ). Both PP2 and PP6 transplantations resulted in more dystrophin-positive fibers than nontransplanted muscles ( $p=0.024$  and  $0.001$ , respectively) or sham transplanted muscles ( $32 \pm 4$ , standard error,  $p=0.023$  and  $0.001$ ) (Fig. 5E).

Human donor cells from both preplate fractions appear to contribute to dystrophin-positive myofibers primarily through fusion with host fibers. The mean fiber diameters were not significantly different compared with the dystrophin-negative fibers in the nontransplanted/no injection muscles (PP2:  $34 \pm 6 \mu\text{m}$ , PP6:  $40 \pm 8 \mu\text{m}$ , and Host:  $39 \pm 15 \mu\text{m}$ , Fig. 6A). Similarly, the mean fiber cross-sectional areas of dystrophin positive fibers resulting from PP2 or PP6 transplantations were not significantly different from host fibers in nontransplanted muscle (PP2:  $1030 \pm 420 \mu\text{m}^2$ , PP6:  $1430 \pm 650 \mu\text{m}^2$ , and Host:  $1130 \pm 660 \mu\text{m}^2$ , Fig. 6B). In rare instances, we observe small dystrophin positive fibers that could indicate *de novo* myofiber formation. We also examined centro-nucleation in the mdx/SCID host muscles and in muscles transplanted with PP2 or PP6 cells. In all cases, there were 55%–60% fibers with central nucleation and no significant difference among the groups (Fig. 6C). We further confirmed the donor cells' participation in skeletal muscle

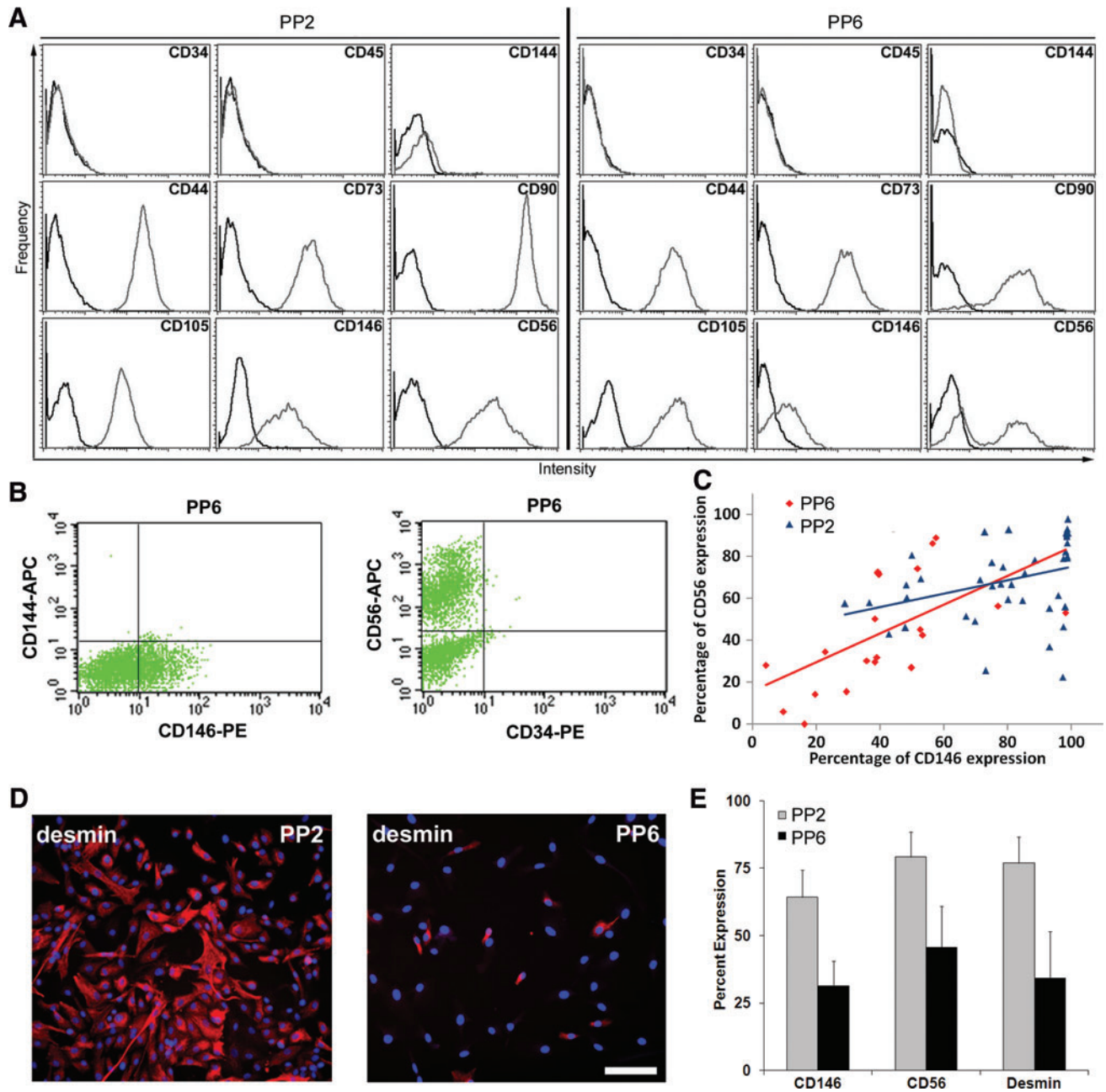


**FIG. 2.** *In vitro* comparison of PP2 and PP6 muscle-derived populations. **(A)** Flow cytometric histograms for PP2 and PP6 populations; cells are negative for CD34, CD45, and CD144; highly positive for CD44, CD73, CD90, and CD105; and exhibit variable expression of CD56 and CD146. **(B)** Flow cytometry dot plots of expression of CD146 and CD56 in slowly adhering populations. The low level of CD146 is visible on the dot plot (CD144 is also shown here), whereas 2 distinct populations of CD56 [+] and CD56 [-] cells are visible on the plot (separate plot with CD34 expression). **(C)** For both PP6 and PP2 populations, there is a significant positive correlation between the level of expression of CD146 and the myogenic marker CD56. **(D)** Immunocytochemistry for desmin expression (red), with Hoechst-labeled nuclei (blue). **(E)** Mean *in vitro* expression of CD56 (flow), CD146 (FACS), and desmin (immunocytochemistry) for PP2 and PP6 populations. Color images available online at [www.liebertonline.com/tea](http://www.liebertonline.com/tea)

regeneration by utilizing a human-specific dystrophin antibody and latex fluorescent beads, which co-localized with the site of cell delivery. Comparisons of serial sections showed that the polyclonal antibody resulted in more intense staining (Fig. 6D) than the human specific DYS3 antibody (Fig. 6E). Finally, we confirm donor-host fusion by detection of host Y-chromosomes present in human dystrophin posi-

tive fibers (Fig. 6F), which shows that female donor cells fuse with host fibers to restore dystrophin. The overall level of dystrophin restoration by the human populations is lower than our previous reports with mouse myoblasts and MDSCs,<sup>21,53</sup> and this may be that the preplate methods to isolate potent muscle cells do not exactly translate in human muscle tissue. In addition, the reduced dystrophin level after

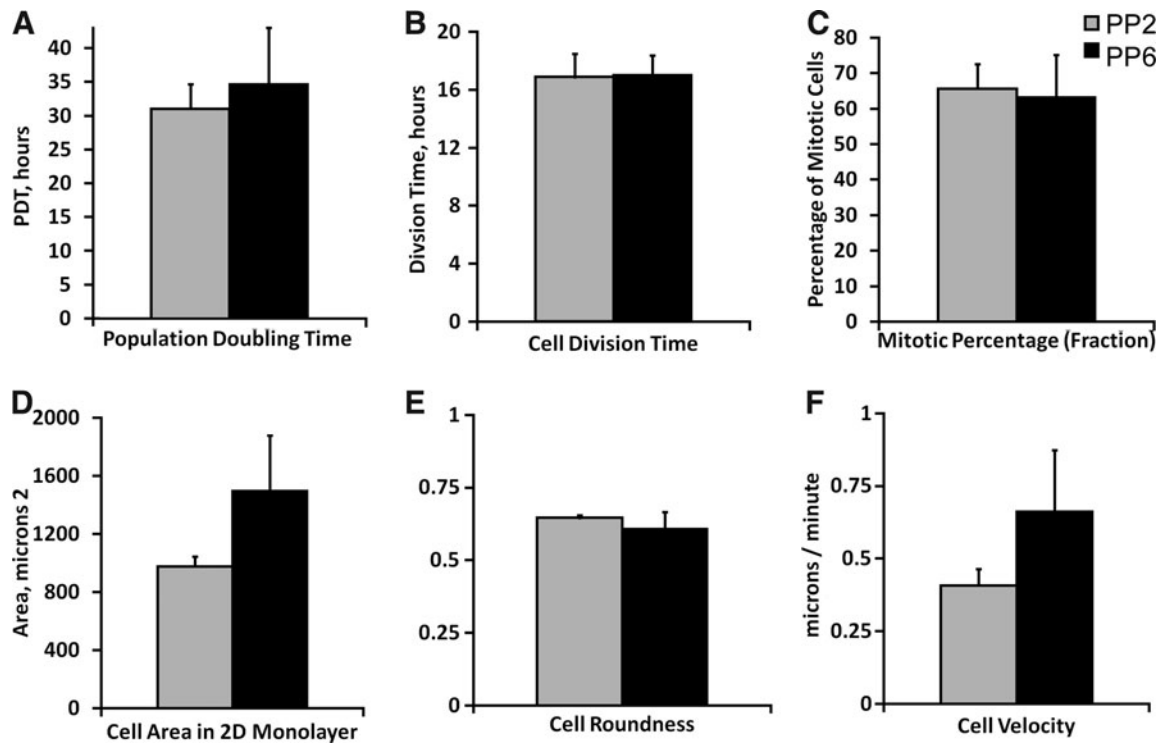


**FIG. 3.** (A–C) Growth characteristics of PP2 and PP6 described by (A) population doubling time (PDT), (B) division time (DT), and (C) mitotic fraction. There were no significant differences in the growth rates between the different fractions; however, the PP6 population had a slight trend toward slower PDT (35 h) as compared with PP2 populations (30 h). (D–F) *In vitro* morphology and migration analysis. PP2 and PP6 cells described by mean cell area or spreading, circularity, and centroid velocity. PP2 cells were significantly larger than PP2 cells, but showed no difference in cell shape or cell roundness. We also found that PP2 were significantly less migratory than PP6 (as measured by cell velocity).

transplantation is likely attributable in part to limitations associated with xenotransplantation. Human cells may be challenged to survive albeit an SCID mouse, and are likely less able to fuse with mouse myofibers, or there may be poor dystrophin integration into the plasma membrane of hybrid

myofibers. Nevertheless, we detect significant differences due to human cell transplantation as compared with no transplantation or sham transplantation.

Although numerous studies describe the msMDSCs as a potential candidate for cell therapy for skeletal muscle for

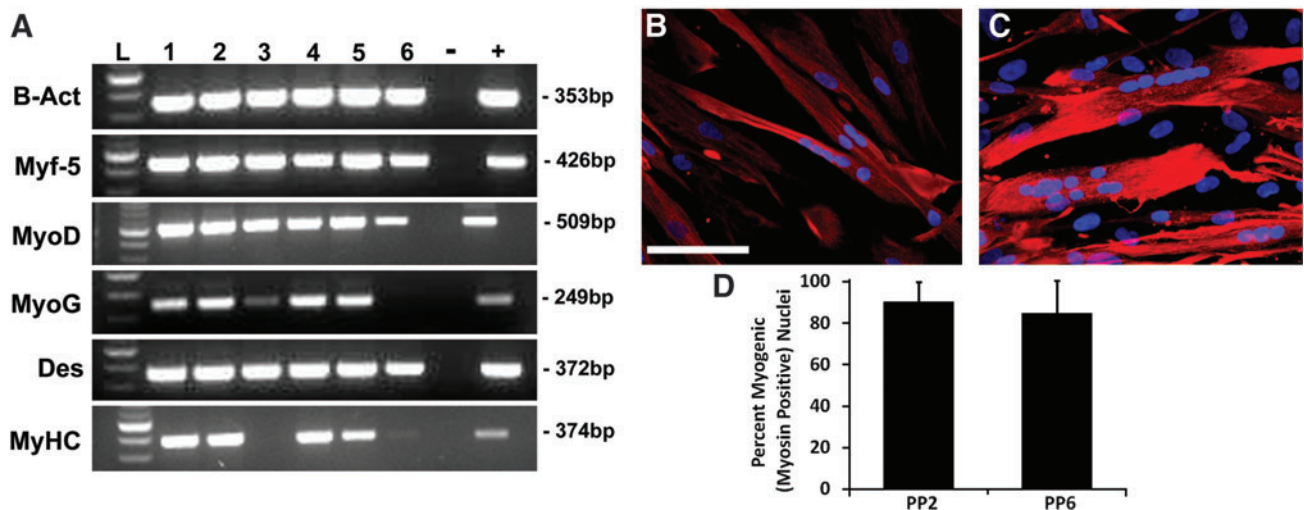


**FIG. 4.** *In vitro* myogenic characterization. (A) RT-PCR of 3 populations of PP2 cells (Lanes 1, 2, and 3), 3 populations of PP6 cells (Lanes 4, 5, and 6), negative control—no cDNA (lane 7), and positive control—human total muscle (lane 8) for myogenic lineage specific markers. (B, C) Fluorescent images of *in vitro* myotubes from PP2 and PP6 populations, respectively, myosin heavy chain in red, nuclei in blue. (D) Quantification of myogenic activity of PP2 and PP6 under myogenic conditions. We detect no significant difference in the percent of myosin positive or fused nuclei between the two populations. Scale bar represents 100  $\mu$ m. RT-PCR, reverse transcription polymerase chain reaction. Color images available online at [www.liebertonline.com/tea](http://www.liebertonline.com/tea)



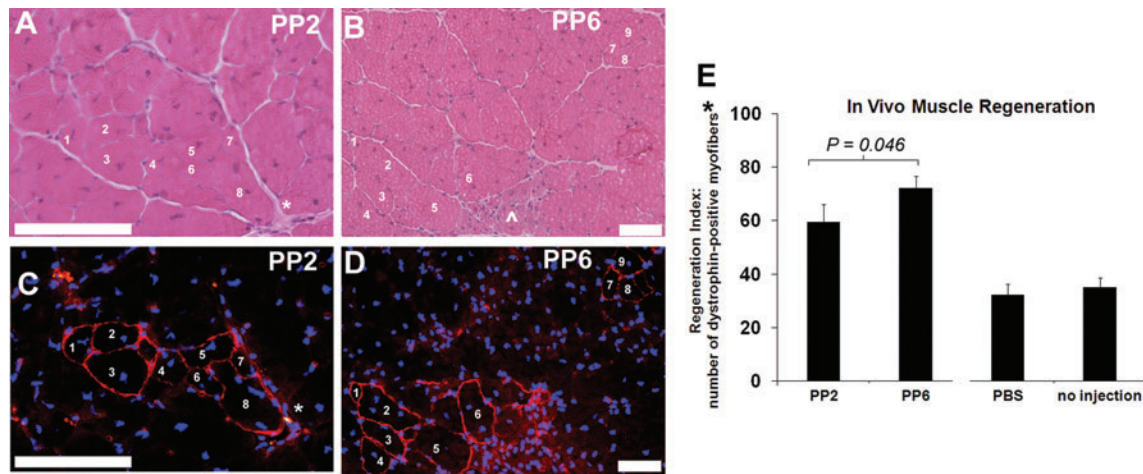


**FIG. 5.** *In vivo* cell participation in muscle regeneration. (A, B) Hematoxylin and eosin stain of transplantation site for PP2 and PP6 populations. Serial section of polyclonal dystrophin antibody (C, D); fluorescent images demonstrate dystrophin positive fibers at 2 weeks post transplantation with PP2 and PP6. (E) Quantification of the level of skeletal muscle regeneration is measured as the regeneration index—number of dystrophin positive fibers per  $10^5$  transplanted donor cells per muscle section. We observe significantly more dystrophin-positive myofibers after PP6 transplantation as compared with PP2 and sham transplantation. \*For PBS and no-injection muscles, no cells were injected; therefore, the y-axis represents only the number of dystrophin-positive fibers. Scale bar represents 100  $\mu$ m. Color images available online at [www.liebertonline.com/tea](http://www.liebertonline.com/tea)

DMD; to date, there have been no studies to examine the translation of this cell type to hMDSCs for skeletal muscle repair. Here, we used the methods developed in murine studies, to determine whether similar function cell types could be isolated from human skeletal muscle. Translating promising mouse studies to humans is necessary; however, it comes with the probability that many aspects will not readily translate. Here, we report both similarities and differences in the mouse and human preplated muscle-derived cells.

The preplate method was used to obtain distinct muscle cell populations based on the different rates of cell adhesion. In previous mouse studies, these different populations were termed “preplates” and described as PP1, PP2, PP3...PP6, where PP1 showed fast adherence, and PP6 showed the slowest adherence.<sup>21</sup> In this study, we compared human PP2 and PP6 cells, as mouse PP2 had been previously described as more committed myoblasts, and PP6 cells had been described as more stem cell-like. Similar to mouse preplate cells, we found greater levels of myogenic markers desmin and CD56 within the myoblast-like PP2 fraction than in the human PP6 fraction. The preplate fractions were nonhomogeneous for these markers in both our human studies here and the mouse studies.<sup>21,25</sup> We also describe for the first time that the human PP6 cells express several mesenchymal stem cell markers including CD90, CD105, CD73, and CD44. *In vitro*, both fractions were able to differentiate to the myogenic lineage.

The most striking difference between the mouse myoblasts and msMDSCs was performance in cell transplantation studies using the *mdx* mice of muscular dystrophy. In this study, we also found a significant difference in the participation of human myoblasts/PP2 as compared with human PP6 cells—the slowly adhering PP6 cells showed a higher level of participation in skeletal muscle repair as compared with the human PP2 myoblasts. We found that the majority of transplanted donor cells fused with host myofibers to give

rise to dystrophin-positive myofibers. The low level of *de novo* myofiber formation, as compared with msMDSC studies, is likely due to the xenotransplantation. This finding supports the notion that human PP6 fraction is the human equivalent of the msMDSC-like fraction and may, therefore, provide a better candidate for cell therapies as compared with more committed myoblasts.

Two aspects of the modified preplate method that remain unresolved in mouse cell studies are (1) how does the modified preplate method purify for MDSCs? and (2) what is the relationship between satellite cells (*in situ*)/myoblasts (*in vitro*) and MDSCs? Since this study demonstrates the use of the preplate method in human tissue, it will be interesting to investigate these questions by using human myoblasts and hMDSCs. In the former case, it remains unknown as to whether the preplate method isolates myoblasts and MDSC populations that initially differ in their cell surface expression of adhesion molecules. It may also be the case that the slowly adhering cells upregulate adhesion molecules during the isolation process, and the adhesion characteristics are secondary to other intrinsic differences between the cells. In this study, both human PP2 and the human PP6 cells expressed similar levels of adhesion molecules as examined by flow cytometry postisolation. We speculate that the preplate method may also separate cells based on different levels of the cells' tolerance to anoikis,<sup>54</sup> or anchorage-independent induced apoptosis. There are several possibilities for which characteristics lead to the cells' separation during the isolation method; however, the majority of msMDSC studies to date have focused on regenerative characteristics of these cells. A more basic understanding of hMDSC-like cells may improve strategies for their efficient isolation and use in transplantation studies, particularly as the preplate method has been used to obtain human myoblasts;<sup>39,55</sup> however, these cells have shown only a limited regeneration capacity in human clinical trials.<sup>12,56</sup>



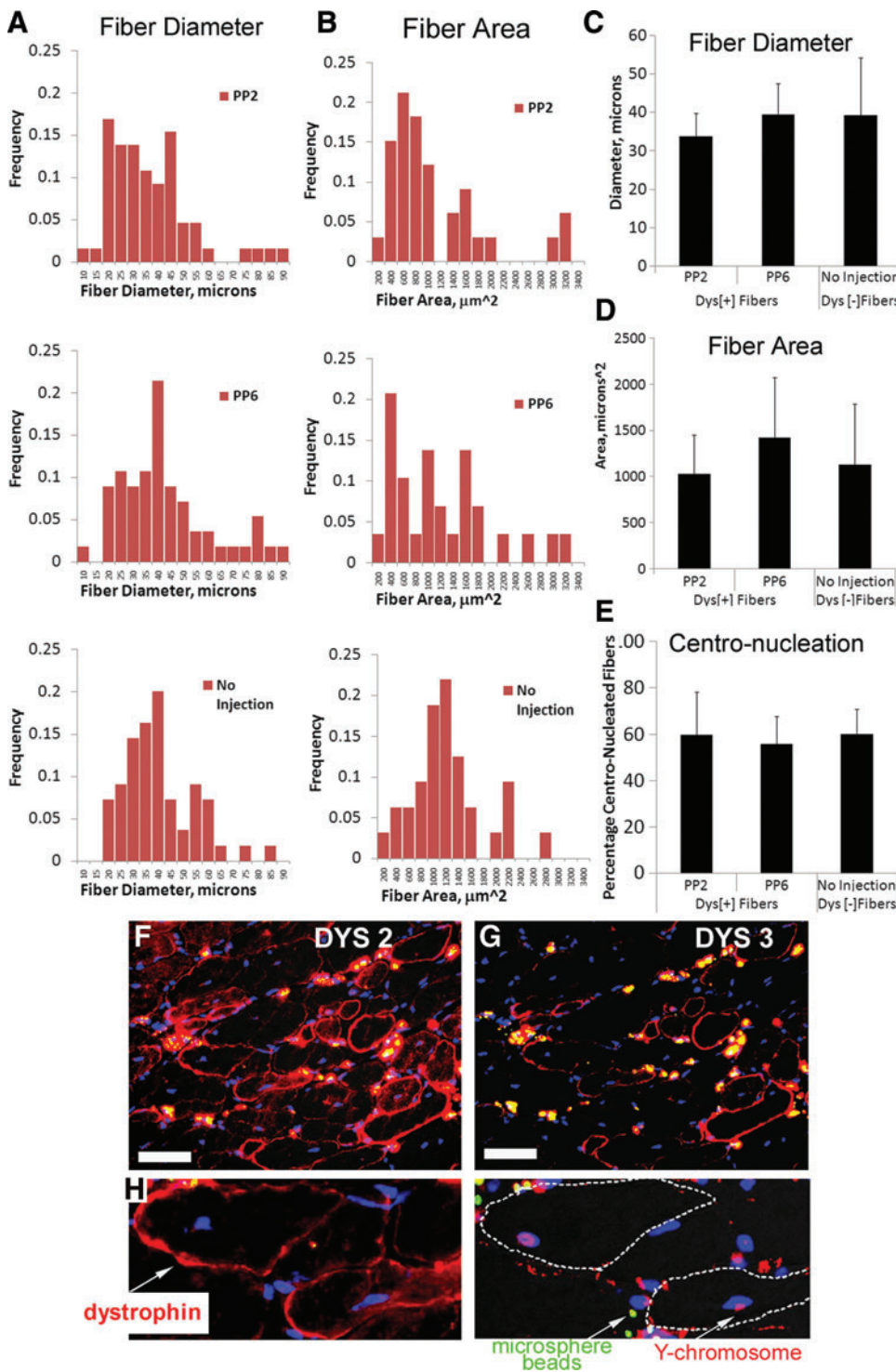


**FIG. 6.** Human cells' contribution to muscle regeneration and fusion with host fibers. **(A)** Histograms of diameters of dystrophin-positive fibers after transplantation of PP2 or PP6, and in muscles with no injection or transplantation. Bins represent fiber sizes 0–10  $\mu\text{m}$ , 10.1–15  $\mu\text{m}$ , 15.1–20  $\mu\text{m}$  etc. **(B)** Histograms of cross-sectional areas of dystrophin-positive fibers after transplantation of PP2 or PP6, and in muscles with no injection or transplantation. Bins represent fiber sizes 0–200  $\mu\text{m}^2$ , 200.1–400  $\mu\text{m}^2$ , 400.1–600  $\mu\text{m}^2$  etc. **(C)** Mean fiber diameter and **(D)** Mean fiber area of dystrophin-positive fibers are similar to host dystrophin-negative fibers. **(E)** Centronucleation in dystrophin-positive fibers is similar to that of the host mdx/SCID fibers. **(F)** and human-specific dystrophin antibody **(G)** show colocalization of the human specific antibody with the microsphere beads used to identify injection site. **(H)** In sex-crossed transplantations, we also detect dystrophin-positive fibers with host male nuclei with Y-chromosome labeling which shows that some donor cells are fusing with host fibers. Scale bar represents 100  $\mu\text{m}$ . Color images available online at [www.liebertonline.com/tea](http://www.liebertonline.com/tea)

Although much research has focused on improving myoblast therapy for the treatment of skeletal muscle disease and injury,<sup>57–59</sup> the use of less committed MDSCs may be an alternative approach. In this regard, a better understanding of the mechanism of myoblast and MDSC separation by preplating will help discern the relationship between these two distinct populations. MDSCs may have a separate origin from satellite cells, as MDSC (like side population cells) appear to be present in Pax 7 knockout mice that are mainly devoid of

satellite cells,<sup>20</sup> though Pax 7 alone has been questioned as a reliable satellite cell marker. Although it has yet to be definitively shown, it has also been hypothesized that MDSCs, and mesenchymal stem cells, may originate from blood vessels, as a subset of msMDSCs express endothelial markers.<sup>7</sup> However, we report here that the PP6 population as a whole expresses low levels of CD146 and CD144.

The mechanism of the preplate method and the relationship of myoblasts and preplate fractions are now questions

that could be examined in human preplate-derived populations. Findings from early human myoblast transplantation trials illustrate the often large disparity in results when moving from non-human animals to human clinical trials. Although the findings here in a DMD SCID mouse implicate the potential development of new therapeutic cells, much work yet remains to better characterize human muscle-derived cells and the dynamic relationship between myoblasts and MDSCs populations.

### Acknowledgments

The authors thank Alison Logar, Samantha L. Sanford, Chris C. Scelfo, and Taylor A. Bissell for technical assistance, and Ron Jankowski and Ryan Pruphnic of Cook Myosite (Harmar PA). This work was supported by the National Institute of Arthritis and Musculoskeletal and Skin Disease (R03 AR053678) and the United States Department of Defense (Grant # W81XWH-06-1-0406).

### Disclosure Statement

None of the authors have any competing financial interests to declare.

### References

- Hoffman, E.P., Brown, R.H., Jr., and Kunkel, L.M. Dystrophin: the protein product of the Duchenne muscular dystrophy locus. *Cell* **51**, 919, 1987.
- Zubrzycka-Gaarn, E.E., *et al.* The Duchenne muscular dystrophy gene product is localized in sarcolemma of human skeletal muscle. *Nature* **333**, 466, 1988.
- Ervasti, J.M., and Campbell, K.P. Membrane organization of the dystrophin-glycoprotein complex. *Cell* **66**, 1121, 1991.
- Bernat, J.L. *Ethical Issues in Neurology*, 3rd edition. Boston: Butterworth-Heinemann. 2008, p. xii, 508.
- Eagle, M., *et al.* Managing Duchenne muscular dystrophy—the additive effect of spinal surgery and home nocturnal ventilation in improving survival. *Neuromuscul Disord* **17**, 470, 2007.
- Rudnicki, M.A., *et al.* The molecular regulation of muscle stem cell function. *Cold Spring Harb Symp Quant Biol* **73**, 323, 2008.
- Peault, B., *et al.* Stem and progenitor cells in skeletal muscle development, maintenance, and therapy. *Mol Ther* **15**, 867, 2007.
- Skuk, D. Myoblast transplantation for inherited myopathies: a clinical approach. *Expert Opin Biol Ther* **4**, 1871, 2004.
- Partridge, T.A., *et al.* Conversion of mdx myofibres from dystrophin-negative to—positive by injection of normal myoblasts. *Nature* **337**, 176, 1989.
- Skuk, D., *et al.* First test of a “high-density injection” protocol for myogenic cell transplantation throughout large volumes of muscles in a Duchenne muscular dystrophy patient: eighteen months follow-up. *Neuromuscul Disord* **17**, 38, 2007.
- Gussoni, E., *et al.* Normal dystrophin transcripts detected in Duchenne muscular dystrophy patients after myoblast transplantation. *Nature* **356**, 435, 1992.
- Huard, J., *et al.* Human myoblast transplantation: preliminary results of 4 cases. *Muscle Nerve* **15**, 550, 1992.
- Karpati, G., *et al.* Myoblast transfer in Duchenne muscular dystrophy. *Ann Neurol* **34**, 8, 1993.
- Huard, J., *et al.* Gene transfer into skeletal muscles by isogenic myoblasts. *Hum Gene Ther* **5**, 949, 1994.
- Kinoshita, I., *et al.* Very efficient myoblast allotransplantation in mice under FK506 immunosuppression. *Muscle Nerve* **17**, 1407, 1994.
- Vilquin, J.T., *et al.* Successful histocompatible myoblast transplantation in dystrophin-deficient mdx mouse despite the production of antibodies against dystrophin. *J Cell Biol* **131**, 975, 1995.
- Mendell, J.R., *et al.* Myoblast transfer in the treatment of Duchenne’s muscular dystrophy. *N Engl J Med* **333**, 832, 1995.
- Skuk, D., *et al.* Dystrophin expression in muscles of duchenne muscular dystrophy patients after high-density injections of normal myogenic cells. *J Neuropathol Exp Neurol* **65**, 371, 2006.
- Cerletti, M., *et al.* Highly efficient, functional engraftment of skeletal muscle stem cells in dystrophic muscles. *Cell* **134**, 37, 2008.
- Lu, A., *et al.* Isolation of myogenic progenitor populations from Pax7-deficient skeletal muscle based on adhesion characteristics. *Gene Ther* **15**, 1116, 2008.
- Qu-Petersen, Z., *et al.* Identification of a novel population of muscle stem cells in mice: potential for muscle regeneration. *J Cell Biol* **157**, 851, 2002.
- Deasy, B.M., *et al.* Long-term self-renewal of postnatal muscle-derived stem cells. *Mol Biol Cell* **16**, 3323, 2005.
- Qu, Z., *et al.* Development of approaches to improve cell survival in myoblast transfer therapy. *J Cell Biol* **142**, 1257, 1998.
- Gussoni, E., *et al.* Dystrophin expression in the mdx mouse restored by stem cell transplantation. *Nature* **401**, 390, 1999.
- Jankowski, R.J., *et al.* Flow cytometric characterization of myogenic cell populations obtained via the preplate technique: potential for rapid isolation of muscle-derived stem cells. *Hum Gene Ther* **12**, 619, 2001.
- Kawada, H., and Ogawa, M. Bone marrow origin of hematopoietic progenitors and stem cells in murine muscle. *Blood* **98**, 2008, 2001.
- McKinney-Freeman, S.L., *et al.* Muscle-derived hematopoietic stem cells are hematopoietic in origin. *Proc Natl Acad Sci USA* **99**, 1341, 2002.
- Pate, D.W., Southerland, B.S., Grande, D.A., Young, H.E., and Lucas, P.A. Isolation and differentiation of mesenchymal stem cells from rabbit muscle. *Clin Res* **41**, 374A, 1993.
- Torrente, Y., *et al.* Intraarterial injection of muscle-derived CD34(+)Sca-1(+) stem cells restores dystrophin in mdx mice. *J Cell Biol* **152**, 335, 2001.
- Williams, J.T., *et al.* Cells isolated from adult human skeletal muscle capable of differentiating into multiple mesodermal phenotypes. *Am Surg* **65**, 22, 1999.
- Jackson, W.M., Nesti, L.J., and Tuan, R.S. Potential therapeutic applications of muscle-derived mesenchymal stem and progenitor cells. *Expert Opin Biol Ther* **10**, 505, 2010.
- Zheng, B., *et al.* Prospective identification of myogenic endothelial cells in human skeletal muscle. *Nat Biotechnol* **25**, 1025, 2007.
- Dellavalle, A., *et al.* Pericytes of human skeletal muscle are myogenic precursors distinct from satellite cells. *Nat Cell Biol* **9**, 255, 2007.
- Torrente, Y., *et al.* Human circulating AC133(+) stem cells restore dystrophin expression and ameliorate function in dystrophic skeletal muscle. *J Clin Invest* **114**, 182, 2004.
- Torrente, Y., *et al.* Autologous transplantation of muscle-derived CD133+ stem cells in Duchenne muscle patients. *Cell Transplant* **16**, 563, 2007.

36. Kim, Y.T., *et al.* Human muscle-derived cell injection in a rat model of stress urinary incontinence. *Muscle Nerve* **36**, 391, 2007.
37. Furuta, A., *et al.* Physiological effects of human muscle-derived stem cell implantation on urethral smooth muscle function. *Int Urogynecol J Pelvic Floor Dysfunct* **19**, 1229, 2008.
38. Carr, L.K., *et al.* 1-year follow-up of autologous muscle-derived stem cell injection pilot study to treat stress urinary incontinence. *Int Urogynecol J Pelvic Floor Dysfunct* **19**, 881, 2008.
39. Rando, T.A., and Blau, H.M. Primary mouse myoblast purification, characterization, and transplantation for cell-mediated gene therapy. *J Cell Biol* **125**, 1275, 1994.
40. Schugar, R.C., *et al.* High harvest yield, high expansion, and phenotype stability of CD146 mesenchymal stromal cells from whole primitive human umbilical cord tissue. *J Biomed Biotechnol* **2009**, 789526, 2009.
41. Deasy, B.M., *et al.* Modeling stem cell population growth: incorporating terms for proliferative heterogeneity. *Stem Cells* **21**, 536, 2003.
42. Deasy, B.M., *et al.* Mechanisms of muscle stem cell expansion with cytokines. *Stem Cells* **20**, 50, 2002.
43. Sarig, R., *et al.* Regeneration and transdifferentiation potential of muscle-derived stem cells propagated as myospheres. *Stem Cells* **24**, 1769, 2006.
44. Arsic, N., *et al.* Vascular endothelial growth factor stimulates skeletal muscle regeneration in vivo. *Mol Ther* **10**, 844, 2004.
45. Hwang, J.H., *et al.* Isolation of muscle derived stem cells from rat and its smooth muscle differentiation [corrected]. *Mol Cells* **17**, 57, 2004.
46. Arsic, N., *et al.* Muscle-derived stem cells isolated as non-adherent population give rise to cardiac, skeletal muscle and neural lineages. *Exp Cell Res* **314**, 1266, 2008.
47. Nolzco, G., *et al.* Effect of muscle-derived stem cells on the restoration of corpora cavernosa smooth muscle and erectile function in the aged rat. *BJU Int* **101**, 1156, 2008.
48. Rouger, K., *et al.* Progenitor cell isolation from muscle-derived cells based on adhesion properties. *J Histochem Cytochem* **55**, 607, 2007.
49. Sun, J.S., Wu, S.Y., and Lin, F.H. The role of muscle-derived stem cells in bone tissue engineering. *Biomaterials* **26**, 3953, 2005.
50. Winitsky, S.O., *et al.* Adult murine skeletal muscle contains cells that can differentiate into beating cardiomyocytes in vitro. *PLoS Biol* **3**, e87, 2005.
51. Sinanan, A.C., Hunt, N.P., and Lewis, M.P. Human adult craniofacial muscle-derived cells: neural-cell adhesion-molecule (NCAM; CD56)-expressing cells appear to contain multipotential stem cells. *Biotechnol Appl Biochem* **40(Pt 1)**, 25, 2004.
52. Deasy, B.M., *et al.* Effect of VEGF on the regenerative capacity of muscle stem cells in dystrophic skeletal muscle. *Mol Ther* **17**, 1788, 2009.
53. Deasy, B.M., *et al.* A role for cell sex in stem cell-mediated skeletal muscle regeneration: female cells have higher muscle regeneration efficiency. *J Cell Biol* **177**, 73, 2007.
54. Ruoslahti, E., and Reed, J.C. Anchorage dependence, integrins, and apoptosis. *Cell* **77**, 477, 1994.
55. Blau, H.M., and Webster, C. Isolation and characterization of human muscle cells. *Proc Natl Acad Sci USA* **78**, 5623, 1981.
56. Skuk, D., *et al.* Dystrophin expression in myofibers of Duchenne muscular dystrophy patients following intramuscular injections of normal myogenic cells. *Mol Ther* **9**, 475, 2004.
57. Brimah, K., *et al.* Human muscle precursor cell regeneration in the mouse host is enhanced by growth factors. *Hum Gene Ther* **15**, 1109, 2004.
58. Bouchentouf, M., *et al.* Vascular endothelial growth factor reduced hypoxia-induced death of human myoblasts and improved their engraftment in mouse muscles. *Gene Ther* **15**, 404, 2008.
59. Mills, P., *et al.* A synthetic mechano growth factor E Peptide enhances myogenic precursor cell transplantation success. *Am J Transplant* **7**, 2247, 2007.

Address correspondence to:  
Bridget M. Deasy, Ph.D.  
Department of Bioengineering  
Swanson School of Engineering  
University of Pittsburgh  
450 Technology Drive  
Pittsburgh, PA 15219

E-mail: deasybm@upmc.edu

Received: September 19, 2010

Accepted: August 19, 2011

Online Publication Date: October 3, 2011